Research Square

Preprints are preliminary reports that have not undergone peer review.
They should not be considered conclusive, used to inform clinical practice,
or referenced by the media as validated information.

# Developing a gelatin-stabilized nanosilver particle/agar hydrogel for visually monitoring the freshness of braised chicken meat

**Ya-lin Peng**
Anhui Agricultural University
**Yong-zhan Wang**
Anhui Agricultural University
**Yu-cong Li**
Anhui Agricultural University
**Li-ting Zeng**
Anhui Agricultural University
**Xin-yi Song**
Anhui Agricultural University
**Xue-qing Li**
Anhui Agricultural University
**Ao-jing Lv**
Anhui Agricultural University
**Rui-ling Dong**
Anhui Agricultural University
**Wen-hao Gao**
Anhui Agricultural University
**Lu Feng**
Anhui Agricultural University
**He-shuai Li**
Anhui Agricultural University
**Jun Qi**
junqi86@hotmail.com
Anhui Agricultural University
**Guo-yuan Xiong**
Anhui Science and Technology University
**Chun-hui Zhang**
Chinese Academy of Agricultural Sciences, Ministry of Agriculture and Rural Affairs

**Article**

**Keywords:** Nano-silver particle/agar hydrogel, Sauce-braised meat, Visual monitoring, Freshness, Color development mechanism

**Posted Date:** July 14th, 2025

**DOI:** https://doi.org/10.21203/rs.3.rs-7034014/v1

**License:** This work is licensed under a Creative Commons Attribution 4.0 International License. Read Full License

**Additional Declarations:** No competing interests reported.

# Abstract

This study developed a novel gelatin-stabilized nano-silver particle/agar hydrogel (AgNP) and explored the color rendering mechanism of AgNP hydrogel in monitoring the freshness of braised chicken. The results showed that the color of AgNP hydrogels shifted from brown to gray-white within 3 days of storage of braised chicken and that AgNP hydrogels extended the shelf-life of unpackaged braised chicken meat from 4 d to 6 d at 4°C ($P < 0.05$). The results of circular dichroism (CD), particle size, zeta potential, and UV indicated that the $Cl^-$ on the surface of braised chicken could react with $Ag^+$ on the surface of AgNP, resulting in the formation of AgCl particles during storage. These AgCl particles were further transformed into black $Ag_2S$ particles, causing the visual color shift of the AgNP to gray-white. Overall, AgNP could provide a new method for the freshness assessment of cooked meat products.


# 1. Introduction

In China, sauce-braised meat products have been consumed for more than 2,000 years and have the largest market share, with an annual consumption of nearly $200 billion [1]. In the manufacture of sauce-braised meat products, meat or by-products are stewed with braised soup, which typically consists of salt, soy sauce, spices, and water [2]. Sauce-braised soup is characterized by repeated use in processing, requiring exogenous additions of salt, spices, and other seasonings at the end of each stewing period. As a result, fresh meat can obtain similar levels of seasoning from the soup that has been repeatedly used during stewing. Further, as a result of repeated use of sauce-braised soup, a large amount of meat-derived flavor substances are enriched in the soup, thereby enhancing the flavor of sauce-braised meat [1]. It is due to this reason that sauce-braised meat products are currently very popular with consumers. Unpackaged sauce-braised meat products, which do not undergo heating sterilization, maintain a high level of flavor quality and enjoy the greatest market share. However, the shelf life of these unpackaged products, especially during the summer, is significantly limited, making freshness a crucial concern.

There are several factors that affect the growth of microorganisms in cooked meat, including sterilization, packaging, storage temperature, and preservatives. In response to consumer demands for eating qualities and clean labels of processed meat, research has focused on extending the shelf life of processed meat by using refrigerator temperatures, modified atmosphere packaging, and natural spices such as rosemary and ginger [3]. According to hurdle technology, the combination of these factors can improve the shelf life of meat products [3,4]. It has also become increasingly popular to use edible films to extend the shelf life of unpackaged meat products. Yuan, et al. [5] have reported that chitosan films can significantly extend the shelf life of fish. Chitosan coating can be employed as active packaging in the meat industry to control postprocessing microbial contaminants, thereby improving the microbial safety of meat products. Currently, edible packaging is primarily applied in the field of ready-to-eat meat products and has not been reported in the field of sauce-braised meat products.

Visual freshness perception is another hot topic in the field of meat quality and safety evaluation. Anthocyanins are widely used to assess the color response of gel films to changes in pH and meat spoilage [6]. As a result of the advancements in active packaging research, food packaging materials that can monitor freshness in real time as well as extend the shelf life of meat are in high demand. Zhang, et al. [7] have reported a novel antibacterial visualized intelligent film for monitoring pork quality by using chitosan to inhibit bacteria as a pH response material. Moreover, a number of other antimicrobial components and color-developing materials were used for the assessment of freshness. Li, et al. [8] have prepared a smart food-packaging material that releases antimicrobials continuously and allows for real-time freshness monitoring. The core of this food film contains a carbon quantum dot derived from citric acid, which can be used as a pH-responsive response of fresh shrimp during the storage period and thus have the capability to detect the freshness of shrimp meat in real-time, while the encapsulated *Artemisia argyi* emission oil extends shelf life. However, these studies focused exclusively on the freshness of raw meat, and the pH of fresh meat increases from 5 to 8 during the storage period; however, the pH of cooked meat undergoes minimal changes throughout its shelf life. As a result, it is important to study a novel antibacterial visualized intelligent film independent of pH response.

The biggest difference between sauce-braised meat products and other boiled meat products is that the soup used for their processing contains a salt content of 3–5%. It has been reported that silver nanoparticles change their morphology from triangular to circular after reacting with chloride ions, while the characteristic peaks of surface plasma resonance absorption of silver nanoparticles were blue-shifted [9]. As a result, the visual appearance of the silver nanoparticle solution may be altered. Moreover, the bacteriostatic properties of silver nanoparticles have a wide range of potential applications in food, and some nanosilver applications have received approval from the US Food and Drug Administration [10]. However, it is still unclear how the changes in surface plasmon resonance spectroscopy of silver nanoparticles can be used to evaluate the freshness of sauce-braised meat products and extend their shelf life. In this experiment, AgNP was synthesized by a one-pot method using gelatin, and AgNP was then immobilized by agar to prepare AgNP hydrogels. Subsequently, AgNP hydrogels were used to visually monitor the freshness of unpackaged sauce-braised chicken meat under 4°C storage, and the color development mechanism and antibacterial effect of AgNP hydrogels were analyzed. The information obtained may provide a mechanism for assessing the freshness of meat products independent of pH response and may be useful for the visual monitoring of unpackaged cooked meat products.

## 2. Materials and methods

## 2.1. Chemicals and reagents

Gelatin (type B, ~ 240 bloom, ≥ 95%) was supplied by Shanghai Aladdin Biochemical Technology Co. Ltd., and polyvinyl pyrrolidone (PVP) was purchased from Shanghai Maclean Biochemical Technology Co. Ltd. All the remaining compounds and solvents used in this study were of analytical grade.

Chicken breasts, which were obtained from fowls (40 days old) when slaughtered, were purchased after slaughter from a local supermarket (RT-Mart, Hefei, China).

## 2.2. Preparation of AgNP

Gelatin particles (1 g) were dissolved in 90 mL of pure water and stirred for 30 min at 60°C to ensure complete dissolution. The gelatin solution was then cooled to room temperature and mixed with 1 g of PVP and 10 mL of 0.1 mol/L silver nitrate solution at 1200 r/min in a dark environment for 10 min. Subsequently, the mixed solution was transferred to a 150-mL conical flask and placed in an autoclave (LX-B100L, Kangmai instrument, Guangdong, China) for 20 min at 121°C. The sample solution acquired after the thermal reaction exhibited a reddish-brown color, and these samples were stored in brown bottles for future use.

## 2.3. Determination of UV–Vis spectroscopy

The UV-Vis spectrum of AgNP was recorded in the range of 300–800 nm using a scanning multi-well spectrophotometer (SpectraMax M2e, Molecular Devices, Sunnyvale, CA, USA).

## 2.4. The antimicrobial activity of AgNP

The antibacterial activity of AgNP was evaluated using the Oxford Cup Method with modifications, as described by Feng, et al. [11]. Gram-positive bacteria (*S. aureus* and *B. subtilis)* and Gram-negative bacteria (*E. coli*) were selected and incubated in Luria-Bertani (LB) liquid medium at 37°C for 24 h. The bacterial culture (0.1 mL, approximately $10^6$ CFU/mL) was inoculated on LB plates. After solidifying the plates, Oxford cups with a diameter of 8 mm were placed, followed by the addition of 150 μL of the AgNP sample. Distilled water was used as a control. The sample on the plate was allowed to diffuse for 1 h and then incubated at 37°C for 24 h. The antibacterial activity of AgNP was evaluated by measuring the average diameter of the circular antibacterial zone using a Vernier caliper.

## 2.5. Preparation of AgNP hydrogel

A 2-g aliquot of agar powder was added to 100 mL of AgNP solution and heated at 80 ℃ for 10 min on a magnetic stirrer at 1200 r/min to ensure complete dissolution of the agar powder. After ultrasonic degassing, 30 mL of the mixed solution was poured into a polystyrene petri dish with a diameter of 90 mm, and the AgNP hydrogel was obtained after solidification at ambient temperature.

## 2.6. Application of AgNP hydrogels on the surface of chicken

Generally, the salt content of braised soup that is used for stewing meat in the processing of sauce-braised meat products is between 3% and 5%. Therefore, in order to simulate the stewing process of braised soup, a series of solutions containing 3%, 4%, and 5% NaCl were used in the experiment to stew fresh chicken breast meat (RT-Mart, Hefei, China). Fresh chicken breast meat was cut into small pieces measuring 2.5cm in length, 2.5cm in width, and 0.5cm in height. To ensure that the meat pieces were completely edible, the meat pieces were placed in NaCl solutions containing 0%, 3%, 4%, and 5%,

respectively. Meanwhile, the meat pieces cooked in distilled water were set as a blank group. Subsequently, on a sterile operating table, the cooked meat was taken out with sterilized tweezers, and its surface moisture was absorbed using filter paper. Finally, the meat pieces were placed on a 4-cm square of AgNP hydrogel in disposable petri dishes. According to the sodium chloride content during stewing, the meat samples exposed to AgNP hydrogel were named AH-0%, AH-3%, AH-4%, and AH-5%, respectively. These disposable petri dishes were stored at 4 ℃ for 7 d.

## 2.7. Color evaluation of AgNP hydrogels

L* (brightness), a* (+, red; -, green), and b* (+, yellow; -, blue) of AgNP hydrogels were measured using a chromameter (CR-400, Konica Minolta Inc., Tokyo, Japan). A standard whiteboard ($L^*_0$=92.91; $a^*_0$=-0.51; $b^*_0$=5.52) was used for calibrating the colorimeter and served as the background for measurements. Five random measurement points were determined on each AgNP hydrogel, and the CIE L*a*b* color coordinates were recorded as the average of these 5 points of data. Meanwhile, the appearance of AgNP hydrogels was observed with a digital camera.

## 2.8. Total aerobic microbial count measurement

Total aerobic microbial counts of chicken samples were conducted according to Katiyo, et al. [12]. Chicken meat (1 g) was placed in a sterile bag (Bkman Biological, Hunan, China) and homogenized with 9 mL of 0.1% sterilized peptone water (Basal Media, Shanghai, China). Subsequently, 0.1 mL of serial decimal dilutions of homogenates was spread on Plate Count Agar (PCA, Merck, Darmstadt, Germany) for incubation at 37°C for 48 h. The results were expressed as log CFU/g.

## 2.9. Total volatile basic nitrogen test (TVB-N)

TVB-N was conducted according to the micro-diffusion method of Chinese National Standard Method GB 5009.228–2016. Briefly, 5 g of ground chicken meat was mixed with 100 mL of distilled water in a beaker and shaken for 30 min at room temperature. The mixture was then filtered through filter paper. Next, 1 mL of the filtrate and 1 mL of saturated $K_2CO_3$ were added to the outer chamber of the diffusion plate, and 1 mL of 20 g/L $H_3BO_3$ solution and 1 drop of mixed indicator (1 part of 1 g/L $C_{15}H_{15}N_3O_2$ solution and 5 parts of 1 g/L $C_{21}H_{14}Br_4O_5S$ solution) were added in the central chamber of the plate. The diffusion plates were incubated at 37°C for 2 h, followed by cooling to room temperature. Finally, a titration test was performed using a 0.01 mol/L HCl solution. The results were expressed as mg/100 g.

## 2.10. pH analysis

The pH of chicken meat was measured according to Liu, et al. [13] with some modifications. Chicken meat (5 g) was homogenized with 50 mL of distilled water at 8000 r/ min for 2 min. The mixture was then filtered, and the filtrate was collected. The pH of the filtrate was measured using a pH meter (PHS-3C, Shanghai INESA Scientific Instrument Co., Ltd., Shanghai, China).

## 2.11. Anion selectivity analysis

Anion selectivity analysis was performed according to Sangaonkar, et al. [14] with modifications. The AgNP solution (10 mL) was mixed with 100 μL of pure water, 1 M of $Cl^-$, 1 M of $CH_3COO^-$, 1 M of $OH^-$, 1 M of $NO_3^-$, 1 M of $SO_4^{2-}$, and 1 M of $NO_2^-$, respectively. Afterwards, the mixture was allowed to stand for 10 minutes before its UV spectra were measured at 520 nm.

## 2.12. Preparation and structure analysis of the AgNP simulation system

Separate solutions of 1% gelatin, 1% PVP, 0.01 M $AgNO_3$, and a mixture of 1% gelatin and 1% PVP were prepared. These solutions were then placed in an autoclave and reacted at 121°C and 0.12 MPa for 20 min. Subsequently, 2 portions of 10 mL solutions were taken from each solution and mixed separately with distilled water and 100 μL of 1M NaCl solution. These groups were labeled as the NaCl-free gelatin group, the NaCl-containing gelatin group, the NaCl-free PVP group, the NaCl-containing PVP group, the NaCl-free $AgNO_3$ group, the NaCl-containing $AgNO_3$ group, the NaCl-free gelatin and PVP group, and the NaCl-containing gelatin and PVP group. Similarly, a 2% gelatin solution and a 2% PVP solution were prepared separately and subjected to the same autoclave conditions. After the thermal reaction, the 2% gelatin solution and 2% PVP solution were mixed in a ratio of 1:1 to obtain two portions of 10 mL solutions, and these solutions were separately mixed with distilled water and 100 μL of 1M NaCl solution. These groups were labeled as the NaCl-free mixed group of gelatin and PVP and the NaCl-containing mixed group of gelatin and PVP. The effect of NaCl on the particle size and zeta potential of components in the AgNP system was observed.

*Circular dichroism spectroscopy analysis*

Circular dichroism (CD) spectroscopy was employed to assess protein structure within the wavelength range of 190–260 nm. A gelatin solution was diluted to a concentration of 0.125 mg/mL. Subsequently, 100 μL of the diluted solution was introduced into a 0.1-cm quartz cuvette (Hellma, Muellheim, Baden, Germany). A spectrophotometer (Applied Photophysics Ltd., London, England) was utilized with the following settings: a step size of 1 nm, an acquisition time of 0.5 seconds per data point, and a bandwidth of 1 nm. The obtained spectra were averaged over 6 scans, and the mean residue ellipticity (θ) was calculated based on an average value of 115 amino acid residues.

*Particle size and zeta-potential analyses*

Upon dilution of the sample solution 100 times with distilled water, the particle size and Zeta potential of the samples were analyzed and measured using a Zeta potential and nanoparticle size analyzer.

## 2.13. Effects of NaCl and $H_2S$ on the structure of AgNP

In order to determine the effect of NaCl on the structure of AgNP, a series of NaCl solutions with different concentrations (0, 400, 600, 800, and 1000 mM) were added individually in 10 μL portions to 10 mL of

AgNP solution. After shaking for equilibrium, the particle size, zeta potential, UV spectrum, circular dichroism, and visual appearance of the samples were measured.

The effect of $H_2S$ on the structure of AgNP was analyzed according to Zhai, et al. [15]. At ambient temperature, a certain mass of $Na_2S$ solid was weighed and placed in a gas-collecting bottle. Simultaneously, an HCl solution with a molar concentration three times higher than that of the $Na_2S$ solid was prepared. The excess HCl was included to prevent the re-dissolution of $H_2S$ gas into the solution. Subsequently, a 100-mL aliquot of the prepared HCl solution was added to the gas-collecting bottle containing the $Na_2S$ solid, and the bottle was sealed immediately. The $H_2S$ gas generated from the reaction between $Na_2S$ and HCl was introduced into the AgNP solution, which had varying NaCl concentrations, through nitrogen gas bubbling for thorough absorption. The entire experiment reached equilibrium after 1 h of reaction, following which the particle size, zeta-potential, UV spectrum, circular dichroism, and visual appearance.

## 2.14. Statistical analysis

All data are presented as mean ± SD (standard deviation) values of four independent experiments. The analyses of variances were determined by one-way analysis using SAS software (SAS Institute Inc., North Carolina, USA), followed by Duncan's multiple range test at a significance level of $P < 0.05$.

# 3. Results and Discussion

## 3.1. Synthesis of AgNPs

Surface plasmon resonance absorption can occur when light illuminates the surface of metal nanoparticles at a frequency that matches the natural oscillation frequency of the metal particles [16]. As a result of this resonance, light is absorbed by metal nanoparticles, and the characteristics of the absorption curve and the maximum absorption wavelength are closely related to the shape of the nanoparticles [17]. As shown in Fig. 1a, the synthesized solution was reddish brown, and its UV-absorption spectra showed a strong absorption peak at 420–430 nm, while the blank group was colorless and exhibited no absorption peak at 300–800 nm. These results indicated that only one SPR band was observed due to the surface plasmon resonance effect of the synthesized silver nanoparticles. Gelatin can reduce $Ag^+$ ions to $Ag^0$ under high temperature and pressure, and then $Ag^0$ aggregates to form AgNP [18]; only spherical AgNP forms a single SPR band at 420 nm [19]. As a result, the results of Fig. 1 indicated that spherical AgNP were obtained.

## 3.2. Antibacterial effect of AgNP

The Oxford cup method was used to evaluate the antibacterial effect of AgNP. Generally, the larger the diameter of the antibacterial circle, the stronger the antibacterial effect of AgNP. Figure 1b shows the antibacterial activity of AgNP against *Escherichia coli*, *Staphylococcus aureus*, and *Bacillus subtilis*. The

inhibition zone diameters of AgNP for *Escherichia coli*, *Staphylococcus aureus*, and *Bacillus subtilis* were 13.52 mm, 12.68 mm, and 12.48 mm, respectively.

The antibacterial effect of AgNP against Gram-negative bacteria (*E. coli*) was significantly stronger than that of Gram-positive bacteria (*Staphylococcus aureus* and *Bacillus subtilis*), which was attributed to the fact that Gram-positive bacteria have thicker cell walls than Gram-negative bacteria, making it easier for AgNPs to penetrate the cell membrane of Gram-negative bacteria [20]. Additionally, Gram-negative bacteria have a higher negative charge than Gram-positive bacteria (Tavares, et al., 2020), and the AgNP prepared in this experiment had a positive charge. As a result, AgNP combined easier with Gram-negative bacteria, increasing bacterial membrane permeability and causing their death [21].

## 3.3. Effect of storage time of braised chicken meat on the color of AgNP hydrogels

The effects of storage time of braised chicken meat on the visual color and CIE chromaticity coordinates of AgNP hydrogels are shown in Fig. S1 and Table 1, respectively. The results from Fig. S1 showed that the AgNP hydrogels (AH) exposed to air remained reddish-brown at 4°C for 7 days without exhibiting any obvious visual color changes, indicating that gelatin-stabilized AgNP exhibited greater storage stability. The visual color of the AgNP hydrogels (AH-0%) contacted with boiled chicken remained reddish-brown during storage, consistent with the color change observed in AgNP hydrogels alone in the air. In contrast, when the AgNP hydrogels were contacted with braised chicken meat made by cooking with 3%, 4%, and 5% salt solutions, their color changed from reddish-brown to gray-white. These results indicated that the color change in the AgNP hydrogels in contact with braised chicken meat during the storage period was related to the salt content of the solution used for stewing chicken meat.

Table 1
The color parameters of the AgNP hydrogel used to monitor the freshness of chicken.

| Color | Contents | Storage days (d) | | | | | | | |
|---|---|---|---|---|---|---|---|---|---|
| | | 0 | 1 | 2 | 3 | 4 | 5 | 6 | 7 |
| | AH | 50.61 ± 1.08$^{a}$ | 48.00 ± 0.59$^{b, A}$ | 46.31 ± 0.21$^{c, A}$ | 49.99 ± 0.53$^{a, A}$ | 50.61 ± 0.20$^{a, A}$ | 49.42 ± 1.23$^{ab, A}$ | 49.33 ± 0.87$^{ab, A}$ | 50.24 ± 0.33$^{a, A}$ |
| | AH-0% | 50.61 ± 1.08$^{a}$ | 47.01 ± 0.72$^{bcd, B}$ | 48.45 ± 0.70$^{b, A}$ | 47.28 ± 0.60$^{bc, B}$ | 46.28 ± 0.40$^{cd, D}$ | 45.08 ± 0.95$^{d, C}$ | 45.62 ± 2.02$^{cd, B}$ | 47.36 ± 0.67$^{bc, B}$ |
| *L** | AH-3% | 50.61 ± 1.08$^{a}$ | 43.20 ± 0.17$^{b, C}$ | 44.01 ± 1.71$^{b, B}$ | 43.13 ± 0.51$^{b, C}$ | 44.22 ± 0.49$^{b, E}$ | 43.53 ± 0.35$^{b, D}$ | 43.96 ± 0.38$^{b, B}$ | 44.32 ± 0.44$^{b, B}$ |
| | AH-4% | 50.61 ± 1.08$^{a}$ | 46.88 ± 0.63$^{b, B}$ | 47.47 ± 0.95$^{b, A}$ | 46.41 ± 0.34$^{b, B}$ | 47.17 ± 0.02$^{b, C}$ | 47.19 ± 0.91$^{b, B}$ | 49.79 ± 0.88$^{a, A}$ | 49.83 ± 0.66$^{a, A}$ |
| | AH-5% | 50.61 ± 1.08$^{a}$ | 46.2 ± 0.28$^{d, B}$ | 48.39 ± 1.50$^{bc, A}$ | 47.10 ± 1.32$^{cd, B}$ | 49.81 ± 0.28$^{ab, B}$ | 47.68 ± 0.44$^{cd, B}$ | 50.48 ± 0.38$^{a, A}$ | 50.16 ± 1.30$^{ab, A}$ |
| | AH | 13.85 ± 0.49$^{c}$ | 13.14 ± 0.12$^{cd, B}$ | 12.84 ± 0.07$^{d, B}$ | 15.85 ± 0.31$^{b, B}$ | 16.04 ± 0.05$^{b, B}$ | 15.82 ± 0.51$^{b, B}$ | 16.26 ± 0.83$^{b, B}$ | 17.40 ± 0.27$^{a, B}$ |
| | AH-0% | 13.85 ± 0.49$^{d}$ | 16.03 ± 1.37$^{bcd, A}$ | 15.99 ± 1.17$^{cd, A}$ | 17.76 ± 1.44$^{abc, A}$ | 18.32 ± 1.69$^{abc, A}$ | 18.65 ± 1.23$^{a, A}$ | 18.08 ± 1.35$^{abc, A}$ | 18.45 ± 0.19$^{ab, A}$ |
| *a** | AH-3% | 13.85 ± 0.49$^{a}$ | 7.41 ± 0.07$^{b, C}$ | 4.34 ± 1.35$^{c, C}$ | 2.99 ± 0.06$^{d, D}$ | 2.88 ± 0.12$^{d, D}$ | 3.04 ± 0.06$^{d, D}$ | 3.11 ± 0.04$^{d, D}$ | 3.11 ± 0.05$^{d, D}$ |
| | AH-4% | 13.85 ± 0.49$^{a}$ | 6.72 ± 0.04$^{b, C}$ | 4.92 ± 0.54$^{c, C}$ | 5.17 ± 0.70$^{c, C}$ | 4.73 ± 0.04$^{c, C}$ | 4.84 ± 0.13$^{c, C}$ | 4.62 ± 0.29$^{c, C}$ | 4.77 ± 0.77$^{c, C}$ |

Note: The data is expressed as mean ± SD, lowercase letters (a-f) indicate significant differences within the same column and uppercase letters (A-D) indicate significant differences within the same row ($P < 0.05$).

| Color | Contents | Storage days (d) | | | | | | | |
|---|---|---|---|---|---|---|---|---|---|
| | | 0 | 1 | 2 | 3 | 4 | 5 | 6 | 7 |
| | AH-5% | 13.85 ± 0.49$^{a}$ | 7.40 ± 1.22$^{b, C}$ | 4.83 ± 0.54$^{c, C}$ | 4.93 ± 0.23$^{c, C}$ | 4.66 ± 0.03$^{c, C}$ | 5.04 ± 0.02$^{c, C}$ | 4.77 ± 0.03$^{c, C}$ | 5.07 ± 0.25$^{c, C}$ |
| | AH | 48.12 ± 0.56$^{a}$ | 47.23 ± 0.27$^{ab, A}$ | 43.99 ± 0.76$^{c, A}$ | 46.15 ± 0.31$^{b, A}$ | 42.69 ± 0.96$^{cd, A}$ | 41.3 ± 1.62$^{de, A}$ | 41.00 ± 0.75$^{e, A}$ | 38.13 ± 0.52$^{f, A}$ |
| | AH-0% | 48.12 ± 0.56$^{a}$ | 46.07 ± 0.93$^{ab, A}$ | 44.21 ± 1.27$^{bc, A}$ | 41.58 ± 2.59$^{cd, B}$ | 40.57 ± 0.27$^{d, B}$ | 38.17 ± 1.80$^{d, B}$ | 39.12 ± 2.55$^{d, A}$ | 39.40 ± 2.39$^{d, A}$ |
| *b** | AH-3% | 48.12 ± 0.56$^{a}$ | 27.61 ± 0.26$^{b, BC}$ | 19.13 ± 0.99$^{c, C}$ | 17.41 ± 0.23$^{d, C}$ | 16.14 ± 0.42$^{e, D}$ | 15.65 ± 0.36$^{e, D}$ | 15.56 ± 0.13$^{e, B}$ | 14.14 ± 0.20$^{f, C}$ |
| | AH-4% | 48.12 ± 0.56$^{a}$ | 28.85 ± 0.23$^{b, B}$ | 21.76 ± 0.60$^{c, B}$ | 17.99 ± 1.87$^{d, C}$ | 18.39 ± 0.31$^{d, C}$ | 17.66 ± 0.19$^{d, C}$ | 16.98 ± 0.14$^{df, B}$ | 15.60 ± 0.27$^{f, C}$ |
| | AH-5% | 48.12 ± 0.56$^{a}$ | 26.03 ± 2.70$^{b, C}$ | 19.13 ± 0.96$^{c, C}$ | 16.55 ± 0.46$^{d, C}$ | 16.15 ± 0.10$^{d, D}$ | 15.08 ± 0.14$^{de, D}$ | 15.11 ± 0.10$^{de, B}$ | 13.49 ± 0.05$^{de, C}$ |

Note: The data is expressed as mean ± SD, lowercase letters (a-f) indicate significant differences within the same column and uppercase letters (A-D) indicate significant differences within the same row ($P < 0.05$).

The results from Table 1 showed that the L value of the AgNP hydrogels (AH) first decreased significantly ($P < 0.05$), then increased significantly, and finally remained constant for the last 5 days. In general, the L value of samples is positively correlated with their surface moisture. Therefore, the decrease in the L value might be attributed to the evaporation of surface water on the hydrogel surfaces, while the subsequent increase in the L value might be attributed to an increase in the surface moisture caused by the rebalancing of moisture within the hydrogels. However, the L value of these hydrogels varied by about 10% during the 7-day storage period, which was consistent with no significant differences in their visual color. During the storage period, the changes in the L values of the AgNP hydrogels contacted with boiled chicken or braised chicken meat made by cooking with 3%, 4%, and 5% salt solutions were similar to those of the AgNP hydrogels alone in air. As the salt concentration of

boiled chicken solution increased, the L value of the AgNP hydrogels contacted with braised chicken meat at each storage period first decreased significantly and then increased significantly within 5 days of storage, whereas the L value of these hydrogels at each storage time increased significantly within the last 2 days of storage. However, these L values varied between 5% and 10%.

The a* value of the AgNP hydrogels (AH) increased significantly after 3 days of storage, then remained constant for the next 3 days, and increased significantly after 7 days of storage. The gradual oxidation of silver nanoparticles may be responsible for the increase in redness [22]. The change in the a* values of the AgNP hydrogels contacted with boiled chicken meat during the storage period was similar to that of the AgNP hydrogels alone in air, with a value change range of about 15%, which was consistent with no significant differences in their visual color. However, the a* value of the AgNP hydrogels contacted with braised chicken meat made by cooking with 3%, 4%, and 5% salt solutions decreased significantly by about 80% during the first three days of storage and then remained constant. These outcomes were contrary to the trend of redness of the AgNP hydrogels exposed to air and contacted with boiled chicken meat, but were consistent with the brownish discoloration of these hydrogels. These results suggested that salt in braised chicken meat could affect the structure of nanosilver particles in the hydrogels through the surface contact between the meat and the hydrogels, resulting in a significant change in the redness [23].

The b* value of the AgNP hydrogels exposed to air and contacted with boiled chicken meat decreased significantly during the storage period, especially within 3 days of storage. The decrease in yellowness should be due to the oxidation of nanosilver particles [22]. The b* values of the AgNP hydrogels exposed to air and contacted with boiled chicken meat decreased by about 20% during the storage period. However, the b* values of the AgNP hydrogels contacted with braised chicken meat made by cooking with 3%, 4%, and 5% salt solutions decreased significantly by about 65% during the first three days of storage, and then remained constant. The results were consistent with the color changes in the hydrogels from brown to gray-white. Therefore, the results of the yellowness values implied that salt in braised chicken meat had a substantial effect on the structure of nanosilver particles in the hydrogels through surface contact [23].

Together with the results of L, a*, and b* values and the visual color changes, the AgNP hydrogels contacted with braised chicken meat made by cooking with 3%, 4%, and 5% salt solutions showed significant color changes during the first 3 days of storage. Generally speaking, the selling period of fresh, unpackaged braised meat products should not exceed 1–3 days at 4°C, since the flavor of braised meat products will be greatly diminished if the shelf life is extended beyond that. As a result, the AgNP hydrogels prepared in this experiment were able to monitor the freshness of braised chicken meat stored at 4°C.

## 3.4. Effect of AgNP hydrogels on the total aerobic microbial counts of braised meat

The effect of the AgNP hydrogels on the total aerobic microbial counts of braised chicken meat is shown in Fig. 2a. As the storage time increased, the total aerobic microbial counts of braised chicken meat from different treatment groups increased significantly, particularly during the first 4 days of storage. The total aerobic microbial counts of braised chicken meat in contact with the AgNP hydrogels were significantly lower than those of braised chicken meat without contact with the AgNP hydrogels after 2 days of storage ($P < 0.05$). However, there were no significant differences in the total aerobic microbial counts of braised chicken meat made by cooking with different salt content solutions ($P > 0.05$). According to the Chinese National Standard GB 2726 – 2016, the total aerobic microbial counts of braised chicken meat should be less than 50,000 CFU/g (4.70 log CFU/g). The total aerobic microbial counts of braised chicken meat from the control group reached the specified limit on the 4th day, while the total aerobic microbial counts of braised chicken meat in contact with the AgNP hydrogels exceeded the limit on the 6th day. This outcome suggested that AgNP hydrogels played a role in inhibiting microbial growth, which was consistent with the results reported by Mathew, et al. [24] that nanocomposite pouches reinforced with silver nanoparticles demonstrated a retardation in the microbial growth of chicken sausage during the storage period.

## 3.5. Effect of AgNP hydrogels on the total volatile basic nitrogen (TVB-N) of braised meat

Total volatile basic nitrogen is used to evaluate the production of basic nitrogen substances, such as cadaverine, putrescine, tyramine, spermine, and ammonia, which are generated by decarboxylation and deamination reactions of proteins caused by microbial growth during storage [25]. Figure 2b shows the effect of AgNP hydrogels on TVB-N levels in braised chicken meat. The TVB-N value of freshly prepared boiled or braised chicken meat from different treatment groups ranged between 13.3 mg/100 mg and 12.6 mg/100 mg, and the TVB-N value increased significantly as the storage time increased ($P < 0.05$). The TVB-N value of boiled chicken meat from the control group reached 24.73 mg / 100 g after 7 days of storage, and the TVB-N value of boiled and braised chicken meat in contact with the AgNP hydrogels was significantly lower than that of the control group. However, the TVB-N value of boiled chicken meat (AH-0%) was significantly higher than that of braised chicken meat (AH-3%, AH-4%, and AH-5%), which might be due to the antibacterial effect provided by the higher osmotic pressure of sodium chloride [26]. Together with the results of the total aerobic microbial counts, it suggested that AgNP hydrogels inhibited the microbial growth of braised meat products despite only surface-to-surface contact.

## 3.6. Selective response of AgNP hydrogels to inorganic anions

The effect of AgNP hydrogels on the pH of chicken meat is shown in Fig. 2c. With the increased storage time, the pH value of chicken meat from different treatment groups increased significantly ($P < 0.05$). The increase in pH could be attributed to an increase in the content of basic amines caused by the

growth of bacteria on the surface of chicken meat [12]. After 3 days of storage, the pH of boiled chicken meat from the control group was significantly higher than that of braised chicken meat in contact with AgNP hydrogels ($P < 0.05$). Among those chicken meat exposed to the AgNP hydrogels, the pH values of boiled chicken meats (AH-0%) were significantly higher than those of braised chicken meat (AH-3%, AH-4%, and AH-5%). However, there was no significant difference in pH values between chicken meat made by cooking with 3%, 4%, and 5% salt solutions. These results were similar to those of TVB-N and total aerobic microbial counts.

Currently, there have been a lot of studies focusing on visually monitoring the freshness of meat based on pH variations during storage. In these studies, anthocyanins are typically used to achieve visual color development based on the increasing pH of meat from acidic to basic [27]. However, in this experiment, the pH of braised chicken meat varied between 6.25 and 6.43 during storage, making it unsuitable to rely on pH differences for monitoring the shelf life of braised chicken meat. The key distinction between braised chicken meat and other meat products in processing is that braised soup used for stewing meat contains 3%-5% salt. The results from Table 1 and Fig. S1 showed that braised chicken meat prepared with 3%-5% salt solution could lead to obvious visual color changes in the AgNP hydrogels in contact with the meat within 3 days of storage at 4 ℃, indicating that salt was responsible for the color-responsive freshness behavior of silver nanoparticles.

Figure 3a shows the response relationship between AgNP and common anions present in meat as observed through UV spectra. At an equal molar concentration, AgNP exhibited a significantly stronger response to $Cl^-$ compared to $CH_3COO^-$, $OH^-$, $NO_3^-$, and $SO_4^{2-}$. The response intensity of AgNP towards $Cl^-$ was approximately 8–50 times higher than towards the other ions. This discrepancy might be related to differences in the solubility product constants ($K_{sp}$) between these ions and $Ag^+$ [28]. The solubility product constants of different silver compounds are shown in Table S1. It can be seen that the $K_{sp}$ of AgCl is much higher than that of other silver compounds. These results suggested that $Cl^-$ should be the key anion responsible for the color change observed in silver nanoparticles. Based on these results, it is speculated that $Cl^-$, which migrates within the chicken meat during the braising process, subsequently re-migrates to the surface of the meat during storage, altering the structure of silver nanoparticles, which should cause the visual color change observed in the AgNP hydrogels.

# 3.7. Color-responsive freshness behavior of AgNP hydrogels

## 3.7.1 The structure of gelatin-stabilized nanosilver particles

In order to reveal the role of gelatin, PVP, and silver nitrate in the formation of silver nanoparticles, Table S2 shows the changes in particle size and zeta-potential of these main components after being heated at 121°C for 20 min, as well as the changes in particle size and potential of the prepared components

upon reacting with NaCl. The heating conditions were consistent with the preparation of the silver nanoparticles. The heat-treated gelatin and PVP were negatively charged, and the heat-treated silver nitrate was positively charged. However, the heat-treated silver nitrate did not exhibit the typical UV spectrum characteristic of silver nanoparticles (data not shown). This outcome indicated that silver nitrate alone did not form silver nanoparticles due to the absence of a reducing agent. The particle size of silver nanoparticles prepared in this experiment was 23.80 nm, with a zeta potential of 13.38 mV (Figs. 4c and 4d). Therefore, it could be concluded that the positive charge of silver nanoparticles originated solely from $Ag^+$ on the surface of silver nanoparticles. Besides, the zeta potential of silver nitrate was 2.3 times higher than that of the silver nanoparticles, indicating that part of $Ag^+$ was reduced to $Ag^0$ in the presence of gelatin [29].

PVP is known to contain numerous polar groups on its polyethylene skeleton [30]. It is commonly used as a stabilizer for hydrophilic particles. The particle size of the heat-treated PVP was approximately 58% of the particle size of the heat-treated gelatin, and the particle size of the mixture of PVP and gelatin after heat treatment was significantly larger than that of the heat-treated PVP but still considerably smaller than that of the heat-treated gelatin. The polar groups present in PVP have the capability to form hydrogen bonds with the proline residues of gelatin [31], leading to the incorporation of PVP within the three-dimensional structure of gelatin and altering the overall structure of gelatin. As a result, a more compact gelatin aggregate was formed. Besides, the zeta potential of PVP and gelatin complex after heat treatment was significantly lower than that of heat-treated gelatin, which also proved that PVP altered the structure of gelatin when PVP was enveloped by gelatin.

Salt can induce conformational changes in proteins by altering electrostatic interactions and acting as negatively charged residues to form salt bridges between carboxyl groups [32]. After adding NaCl, the particle size of heat-treated gelatin increased significantly ($P < 0.05$), and the absolute zeta potential value decreased significantly ($P < 0.05$), suggesting that the addition of NaCl resulted in the shielding of electrostatic interactions between ionizing groups on the molecular chain of gelatin and an increase in the aggregation of gelatin. Sow and Yang [33] reported that the addition of a 1.5% NaCl solution caused a structural transition in fish gelatin from an ordered to a disordered structure, resulting in a decrease in helix level and an increase in random coil level. Similarly, the particle size of PVP increased significantly from 15.87 nm to 25.63 nm ($P < 0.05$) after the addition of NaCl, which may be due to salting-out [34]. For $AgNO_3$, the addition of NaCl caused $Ag^+$ to readily react with $Cl^-$, resulting in the formation of AgCl precipitation particles in the suspension and a significant increase in the particle size ($P < 0.05$). After the addition of NaCl, the particle size of these substances increased by approximately 25%-60%, while the particle size of silver nanoparticles increased by 172% under the same NaCl conditions (Fig. 4c). These outcomes indicated that the increased particle size of silver nanoparticles was due to the formation of AgCl through the reaction between $Ag^+$ and $Cl^-$ on the surface of the silver nanoparticles, as well as the aggregation of the gelatin and PVP complex induced by NaCl.

## 3.7.2 Color-responsive freshness behavior of gelatin-stabilized silver nanoparticles

In order to reveal the color-responsive freshness behavior of AgNP hydrogels in contact with braised chicken meat during cold storage, the effects of $Cl^-$ and $H_2S$ on the structure of gelatin-stabilized silver nanoparticles were investigated, because $H_2S$ is also an important index affecting the color development of silver nanoparticles. Figure 4 shows the effect of NaCl concentration on the appearance, UV spectrum, particle size, zeta potential and circular dichroism of AgNP solution.

The result of Fig. 4a suggested that the UV absorption increased with the increase in the $Cl^-$ content. The increase in the absorbance value could be attributed to the reaction between $Cl^-$ and $Ag^+$ on the surface of AgNP, leading to the formation of AgCl precipitation [35]. These precipitates adhered to the surface of AgNP, creating a "black hole" effect that enhanced the UV absorbance. Besides, the half-peak width of UV-absorption spectra is indicative of particle size uniformity [36]. A narrower half-peak width and better symmetry correspond to a more uniform particle size distribution of the synthesized AgNP. With the increase in the $Cl^-$ content, the uniformity of AgNP decreased (Fig. 4a), which was consistent with the result that the original spatial structure of AgNP was destroyed by the reaction between $Cl^-$ and $Ag^+$ on the surface of AgNP.

In this experiment, the average particle size of AgNP synthesized by the one-pot method was 23.80 ± 3.53nm (Fig. 4c). PVP could interact with hydrophilic groups of gelatin and was embedded within the gelatin matrix, providing steric hindrance. The hydrophobic groups of gelatin could interact with hydrophobic silver nanoparticles. These effects were critical for the stability of AgNP prepared by the one-pot method. As the NaCl concentration increased, the particle size of AgNP increased significantly ($P < 0.05$), from 23.80 nm to 64.86 nm (Fig. 4c). The results from Fig. 4d indicated that the zeta potential of AgNP decreased significantly from 13.83 mV to 0.55 mV with the increased NaCl concentration ($P < 0.05$). The results of zeta potential and particle size suggested that the reaction between $Cl^-$ and $Ag^+$ on the surface of AgNP decreased the surface charge of AgNP due to charge neutralization. This decrease in the electrostatic repulsion among AgNP led to the aggregation and larger particle size of AgNP, as well as a decrease in the stability of AgNP, since electrostatic interaction is an important force to maintain the spatial structure of AgNP [37]. These results were consistent with those of the UV spectra.

UV-CD spectroscopy was used to analyze the effect of NaCl on the secondary structure of gelatin in AgNP, as shown in Fig. 4e. The results revealed two distinct peaks in the CD spectrum: a positive peak at 220 nm and a negative peak at 199 nm, which was in line with the typical CD spectrum characteristics of gelatin [38]. As the NaCl concentration increased, the absolute value of the negative peak decreased significantly, while there was no significant difference in the absolute value of the positive peak at 220 nm. A decrease in the absolute value of the negative peak of the CD spectrum of gelatin indicates an enhanced aggregation of gelatin molecules. As a result, this finding suggested that gelatin molecules

exhibited a higher degree of aggregation as the NaCl concentration increased, which was consistent with the results of Zeta potential, particle size, and UV spectrum.

Figure 5 shows the effect of $H_2S$ on the appearance, UV spectrum, particle size, zeta potential and circular dichroism of the NaCl-AgNP solution described in the previous section. When a certain concentration of $H_2S$ gas was injected into the NaCl-AgNP solution, the absorbance value of the maximum absorption peak at 420 nm significantly increased with the increased NaCl concentration (Fig. 5a), and the visual appearance of the solution gradually transformed from transparent yellow to gray (Fig. 5b). The solubility product constants of $Ag_2S$ and AgCl are $6.3*10^{-50}$ and $1.8*10^{-10}$, respectively. It can be seen that the solubility product constant of $Ag_2S$ is considerably lower than that of AgCl. Consequently, in the presence of $H_2S$, $HS^-$ and $S^{2-}$, the AgCl on the surface of AgNP underwent a transformation into black $Ag_2S$ [39].

The formation of the $Ag_2S$ layer on the AgNP surface significantly altered the extinction characteristics of the surface plasmon resonance spectroscopy of AgNP, and the NaCl concentration played a crucial role in modifying the visual color of the $Ag_2S$ layer (Fig. 5b), which were consistent with the findings reported by Estrada-Mendoza, et al. [40]. After the injection of $H_2S$, the particle size of AgNP further increased to 116.63 nm from 64.87 nm ($P < 0.05$), and the Zeta potential decreased significantly, indicating that the stability of synthesized AgNP further deteriorated under the influence of $H_2S$. Upon the addition of NaCl, the absolute value of the negative peak value of the CD spectrum of gelatin decreased significantly, but there was no significant difference in the absolute value of the negative peak value when NaCl concentration increased. Subsequently, when $H_2S$ was introduced, the absolute value of the negative peak of the CD spectrum of gelatin decreased significantly in the presence of NaCl, but there was no significant difference in the absolute value of the negative peak of the CD spectrum of gelatin when NaCl concentration increased.

Briefly, in the one-pot method used in this experiment, gelatin reduced $Ag^+$ ions to $Ag^0$, and the unreduced $Ag^+$ was adsorbed on the surface of $Ag^0$, as well as $Ag^0$ was bound to the hydrophobic residues of gelatin by hydrophobic interaction. Concurrently, PVP became embedded in the three-dimensional structure of gelatin through hydrogen bonding between the carboxyl group of PVP and the proline of gelatin, which played a crucial role in stabilizing the spatial conformation of gelatin. As a result, the gelatin-PVP complex served as a framework for AgNP, with the nanosilver particles being located on this gelatin-PVP skeleton through hydrophobic interactions. During the storage period, NaCl present inside braised chicken meat re-migrated to the surface of the meat and came into contact with the AgNP hydrogels. Subsequently, $Cl^-$ reacted with $Ag^+$ on the surface of AgNP, leading to the formation of AgCl particles attached to the AgNP surface. Simultaneously, NaCl led to the shielding of electrostatic interactions between ionizing groups on the gelatin molecule chains, resulting in an increased aggregation of gelatin molecules and a decrease in the stability of the gelatin-PVP complex. With the extension of storage time, the AgCl particles underwent further transformation into black $Ag_2S$ particles

attached to the surface of AgNP in the presence of $H_2S$ produced by microorganisms, and the gelatin-PVP complex was further aggregated, leading to the visual color of AgNP shifting to gray-white. These processes delineated the mechanism behind the color-responsive freshness behavior of gelatin-stabilized AgNP hydrogels when in contact with braised chicken.

# 4. Conclusions

AgNP was synthesized from gelatin using the one-pot method, and PVP was incorporated into the three-dimensional matrix of gelatin through hydrogen bonding between its carboxyl groups and the proline of gelatin. Due to the antimicrobial properties of AgNP, the shelf life of unpackaged sauce-braised chicken products was extended from 4 to 6 days. Moreover, one notable difference between sauce-braised meat products and other boiled meat products lies in the higher salt content (3%-5%) of the soup used for processing. As a consequence, NaCl present within braised chicken meat re-migrated to the surface of the meat, and $Cl^-$ reacted with $Ag^+$ on the surface of AgNP, forming AgCl particles that attached to the AgNP surface. During storage, AgCl underwent further transformation into black $Ag_2S$ particles in the presence of $H_2S$ produced by microorganisms, and the gelatin-PVP complex was further aggregated, leading to a visual color shift of AgNP to gray-white. This color shift of AgNP served as an indicator of the freshness of braised chicken meat. The research may provide an experimental and theoretical basis for the potential application of AgNP hydrogels in monitoring the freshness of sauce-braised meat products.

**CRediT authorship contribution statement**:

**Ya-lin Peng**: Writing – original draft, Investigation, Formal analysis, Data curation. **Yong-zhan Wang**: Writing – review & editing, Writing – original draft, Validation, Project administration. **Yu-cong Li**: Supervision, Methodology, Investigation. **Li-ting Zeng**: Writing – review & editing, Visualization, Data curation. **Xin-yi Song**: Conceptualization, Validation, Supervision. **Xue-qing Li**: Data curation, Investigation, Conceptualization. **Ao-jing Lv**: Validation, Supervision, Methodology. **Rui-ling Dong**: Validation, Software, Data curation. **Wen-hao Gao**: Validation, Investigation. **Lu Feng**: Validation, Conceptualization. **He-shuai Li**: Supervision, Investigation. **Jun Qi**: Writing – review & editing, Validation, Supervision, Project administration, Methodology, Investigation, Funding acquisition, Conceptualization. **Guo-yuan Xiong**: Validation, Supervision, Project administration, Conceptualization. **Chun-hui Zhang**: Writing – review & editing, Validation, Supervision, Project administration, Conceptualization.

# Declarations

# Declaration of competing interest:

The authors declare that they have no known competing financial interests or personal relationships that could have appeared to influence the work reported in this paper.

# Author Contribution

P.: Writing – original draft, Investigation, Formal analysis, Data curation. W.: Writing – review & editing, Writing – original draft, Validation, Project administration. L.: Supervision, Methodology, Investigation. Z.: Writing – review & editing, Visualization, Data curation. S.: Conceptualization, Validation, Supervision. L.: Data curation, Investigation, Conceptualization. L.: Validation, Supervision, Methodology. D.: Validation, Software, Data curation. G.: Validation, Investigation. F.: Validation, Conceptualization. L.: Supervision, Investigation. Q.: Writing – review & editing, Validation, Supervision, Project administration, Methodology, Investigation, Funding acquisition, Conceptualization. X.: Validation, Supervision, Project administration, Conceptualization. Z.: Writing – review & editing, Validation, Supervision, Project administration, Conceptualization.

# Acknowledgments

This work was supported by the National Natural Science Foundation of China (32001724), the Outstanding Young Teachers Cultivation Program for Young and Middle-aged Teachers Cultivation Action in Universities in Anhui Province (YQZD2023015), Anhui Graduate Academic Innovation Project (2022xscx047), and the University-level Innovation and Entrepreneurship Training Program for College Students of Anhui Agricultural University (X202310364007).

## References

1. Du, C., Qi, J., Yang, C., Zhang, Q. & Liu, D. Enrichment of taste and aroma perceptions in chicken meat stewed in braised soup used repeatedly. *Journal of Food Science* 87, 2563–2577 (2022). http://doi.org/10.1111/1750-3841.16180
2. Qi, J. *et al.* Enrichment of taste and aroma compounds in braised soup during repeated stewing of chicken meat. *Lwt-Food Science and Technology* 168 (2022). http://doi.org/10.1016/j.lwt.2022.113926
3. Zhou, Y., Li, Z., Chen, Y., Fang, H. & Wang, S. Effects of rosemary and ginger on the storage quality of western-style smoked sausage. *Journal of Food Processing and Preservation* 45, e15634 (2021). http://doi.org/10.1111/jfpp.15634
4. Chen, X. *et al.* Effect of modified atmosphere packaging on shelf life and bacterial community of roast duck meat. *Food Research International* 137, 109645 (2020). http://doi.org/10.1016/j.foodres.2020.109645
5. Yuan, D., Hao, X., Liu, G., Yue, Y. & Duan, J. A novel composite edible film fabricated by incorporating W/O/W emulsion into a chitosan film to improve the protection of fresh fish meat. *Food Chemistry* 385, 132647 (2022). http://doi.org/10.1016/j.foodchem.2022.132647
6. Chen, M. *et al.* Intelligent biogenic pH-sensitive and amine-responsive color-changing label for real-time monitoring of shrimp freshness. *Journal of the Science of Food and Agriculture* 103, 7798–

7808 (2023). http://doi.org/10.1002/jsfa.12856

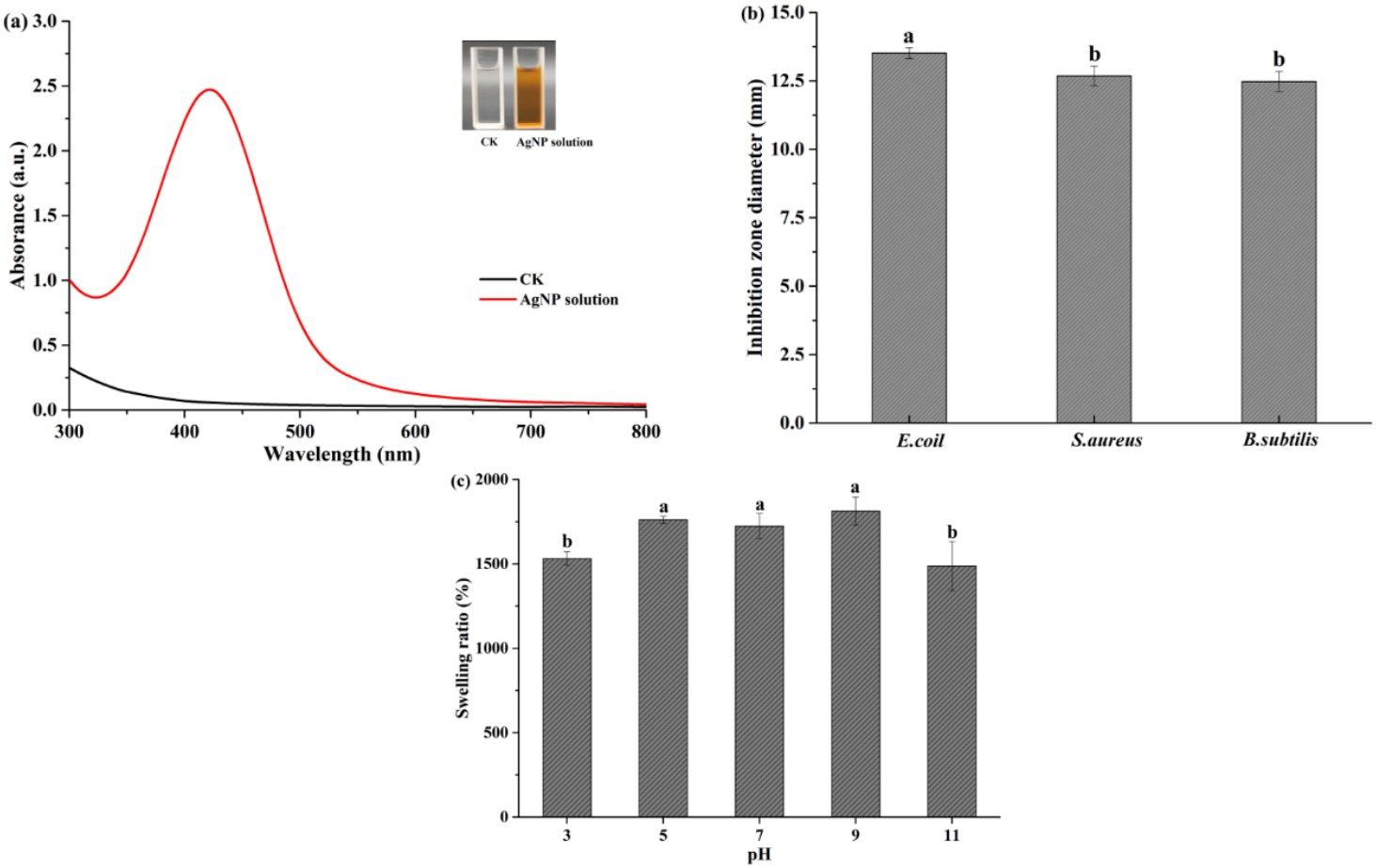
7. Zhang, J. *et al.* Fabrication and characterization of polyvinyl alcohol/sodium alginate/zein/chitosan bilayer film for dynamic visualization of pork quality. *International Journal of Biological Macromolecules*, 125065 (2023). http://doi.org/10.1016/j.ijbiomac.2023.125065
8. Li, C. *et al.* Biobased Intelligent Food-Packaging Materials with Sustained-Release Antibacterial and Real-Time Monitoring Ability. *ACS Applied Materials & Interfaces* 15, 37966–37975 (2023). http://doi.org/10.1021/acsami.3c09709
9. Chen, A. *et al.* Rapid determination of chloride using silver triangular nanoplates. *Analytical Letters* 48, 2223–2233 (2015). http://doi.org/10.1080/00032719.2015.1025276
10. Dunn, K. & Edwards-Jones, V. The role of Acticoat™ with nanocrystalline silver in the management of burns. *Burns* 30, S1–S9 (2004). http://doi.org/10.1016/s0305-4179(04)90000-9
11. Feng, D., Zhang, R., Zhang, M., Fang, A. & Shi, F. Synthesis of eco-friendly silver nanoparticles using glycyrrhizin and evaluation of their antibacterial ability. *Nanomaterials* 12, 2636 (2022). http://doi.org/10.3390/nano12152636
12. Katiyo, W., de Kock, H. L., Coorey, R. & Buys, E. M. Sensory implications of chicken meat spoilage in relation to microbial and physicochemical characteristics during refrigerated storage. *LWT - Food Science and Technology* 128, 109468 (2020). http://doi.org/10.1016/j.lwt.2020.109468
13. Liu, Y. *et al.* A fluorescent pH probe for evaluating the freshness of chicken breast meat. *Food Chemistry* 384, 132554 (2022). http://doi.org/10.1016/j.foodchem.2022.132554
14. Sangaonkar, G. M., Desai, M. P., Dongale, T. D. & Pawar, K. D. Selective interaction between phytomediated anionic silver nanoparticles and mercury leading to amalgam formation enables highly sensitive, colorimetric and memristor-based detection of mercury. *Scientific Reports* 10, 2037 (2020). http://doi.org/10.1038/s41598-020-58844-4
15. Zhai, X. *et al.* A colorimetric hydrogen sulfide sensor based on gellan gum-silver nanoparticles bionanocomposite for monitoring of meat spoilage in intelligent packaging. *Food chemistry* 290, 135–143 (2019). http://doi.org/10.1016/j.foodchem.2019.03.138
16. Semchuk, O. Y., Biliuk, A., Havryliuk, O. & Biliuk, A. Kinetic theory of electroconductivity of metal nanoparticles in the condition of surface plasmon resonance. *Applied Surface Science Advances* 3, 100057 (2021). http://doi.org/10.1016/j.apsadv.2021.100057
17. Kravets, V. G., Kabashin, A. V., Barnes, W. L. & Grigorenko, A. N. Plasmonic surface lattice resonances: a review of properties and applications. *Chemical reviews* 118, 5912–5951 (2018). http://doi.org/10.1021/acs.chemrev.8b00243
18. Azizi-Lalabadi, M., Garavand, F. & Jafari, S. M. Incorporation of silver nanoparticles into active antimicrobial nanocomposites: Release behavior, analyzing techniques, applications and safety issues. *Advances in colloid and interface science* 293, 102440 (2021). http://doi.org/10.1016/j.cis.2021.102440
19. Logaranjan, K., Raiza, A. J., Gopinath, S. C., Chen, Y. & Pandian, K. Shape-and size-controlled synthesis of silver nanoparticles using Aloe vera plant extract and their antimicrobial activity.

*Nanoscale research letters* 11, 1–9 (2016). http://doi.org/10.1186/s11671-016-1725-x

20. Donga, S. & Chanda, S. Facile green synthesis of silver nanoparticles using Mangifera indica seed aqueous extract and its antimicrobial, antioxidant and cytotoxic potential (3-in-1 system). *Artificial cells, nanomedicine, and biotechnology* 49, 292–302 (2021). http://doi.org/10.1080/21691401.2021.1899193
21. Tavares, T. D. *et al.* Activity of specialized biomolecules against gram-positive and gram-negative bacteria. *Antibiotics* 9, 314 (2020). http://doi.org/10.3390/antibiotics9060314
22. Han, Y. *et al.* Effect of oxidation on surface-enhanced Raman scattering activity of silver nanoparticles: a quantitative correlation. *Analytical chemistry* 83, 5873–5880 (2011). http://doi.org/10.1021/ac2005839
23. Ma, Y., Shen, X. F., Liu, F. & Pang, Y. H. Colorimetric detection toward halide ions by a silver nanocluster hydrogel. *Talanta* 211 (2020). http://doi.org/10.1016/j.talanta.2020.120717
24. Mathew, S., Snigdha, S., Mathew, J. & Radhakrishnan, E. K. Biodegradable and active nanocomposite pouches reinforced with silver nanoparticles for improved packaging of chicken sausages. *Food Packaging and Shelf Life* 19, 155–166 (2019). http://doi.org/10.1016/j.fpsl.2018.12.009
25. Bekhit, A. E. D. A., Giteru, S. G., Holman, B. W. & Hopkins, D. L. Total volatile basic nitrogen and trimethylamine in muscle foods: Potential formation pathways and effects on human health. *Comprehensive Reviews in Food Science and Food Safety* 20, 3620–3666 (2021). http://doi.org/10.1111/1541-4337.12764
26. Kim, N. H., Kim, H. W., Moon, H. & Rhee, M. S. Sodium chloride significantly enhances the bactericidal actions of carvacrol and thymol against the halotolerant species Escherichia coli O157: H7, Listeria monocytogenes, and Staphylococcus aureus. *LWT - Food Science and Technology* 122, 109015 (2020). http://doi.org/10.1016/j.lwt.2020.109015
27. Zeng, F., Ye, Y., Liu, J. & Fei, P. Intelligent pH indicator composite film based on pectin/chitosan incorporated with black rice anthocyanins for meat freshness monitoring. *Food Chemistry: X* 17, 100531 (2023). http://doi.org/10.1016/j.fochx.2022.100531
28. Huang, Z. *et al.* Antimicrobial efficacy and mechanisms of silver nanoparticles against Phanerochaete chrysosporium in the presence of common electrolytes and humic acid. *Journal of hazardous materials* 383, 121153 (2020). http://doi.org/10.1016/j.jhazmat.2019.121153
29. Lavanya, K., Kalaimurugan, D., Shivakumar, M. S. & Venkatesan, S. Gelatin stabilized silver nanoparticle provides higher antimicrobial efficiency as against chemically synthesized silver nanoparticle. *Journal of Cluster Science* 31, 265–275 (2020). http://doi.org/10.1007/s10876-019-01644-2
30. Zein, R., Alghoraibi, I., Soukkarieh, C., Ismail, M. T. & Alahmad, A. Influence of polyvinylpyrrolidone concentration on properties and anti-bacterial activity of green synthesized silver nanoparticles. *Micromachines* 13, 777 (2022). http://doi.org/10.3390/mi13050777
31. Pérez-Marroquín, X. A. *et al.* Green Synthesis of Silver Nanoparticles for Preparation of Gelatin Films with Antimicrobial Activity. *Polymers* 14, 3453 (2022). http://doi.org/10.3390/polym14173453

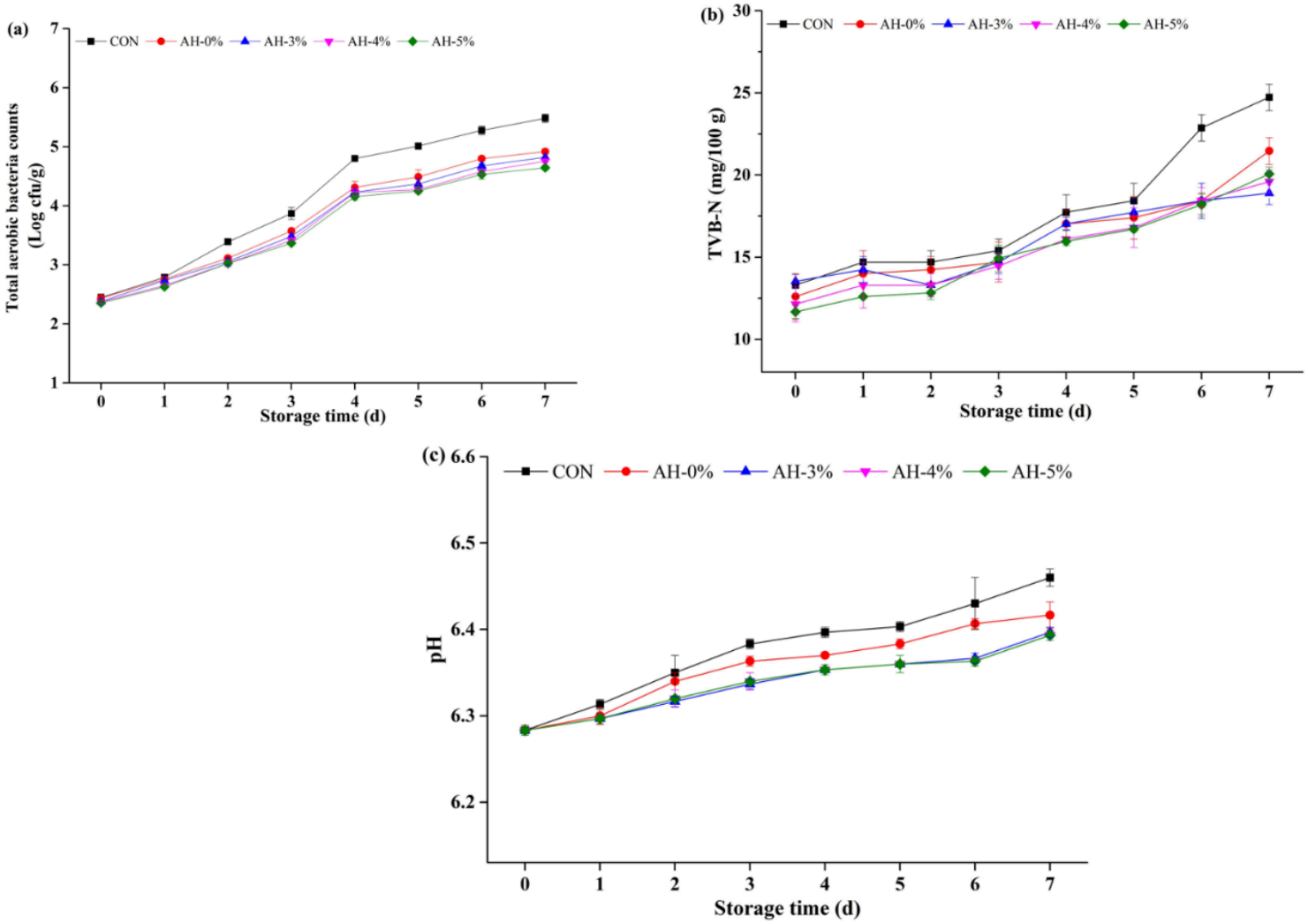
32. Zhao, Y. *et al.* Comparative study on the effect of different salts on surimi gelation and gel properties. *Food Hydrocolloids*, 108982 (2023). http://doi.org/10.1016/j.foodhyd.2023.108982
33. Sow, L. C. & Yang, H. Effects of salt and sugar addition on the physicochemical properties and nanostructure of fish gelatin. *Food Hydrocolloids* 45, 72–82 (2015).
34. Milosavljevic, V. *et al.* Alternative synthesis route of biocompatible polyvinylpyrrolidone nanoparticles and their effect on pathogenic microorganisms. *Molecular Pharmaceutics* 14, 221–233 (2017). http://doi.org/10.1021/acs.molpharmaceut.6b00807
35. Phoonsawat, K., Ratnarathorn, N., Henry, C. S. & Dungchai, W. A distance-based paper sensor for the determination of chloride ions using silver nanoparticles. *Analyst* 143, 3867–3873 (2018). http://doi.org/10.1039/c8an00670a
36. Zeng, Y., Wu, X., Yang, H., Zong, M. & Lou, W. 1, 4-α-Glucosidase from Fusarium solani for Controllable Biosynthesis of Silver Nanoparticles and Their Multifunctional Applications. *International Journal of Molecular Sciences* 24, 5865 (2023). http://doi.org/10.3390/ijms24065865
37. Zhao, J. *et al.* Ionic-strength-dependent effect of suspended sediment on the aggregation, dissolution and settling of silver nanoparticles. *Environmental Pollution* 279, 116926 (2021). http://doi.org/10.1016/j.envpol.2021.116926
38. Qi, J. *et al.* Effect of short-term frozen storage of raw meat on aroma retention of chicken broth: A perspective on physicochemical properties of broth. *LWT - Food Science and Technology* 162, 113480 (2022). http://doi.org/10.1016/j.lwt.2022.113480
39. Yang, Y. *et al.* Environmental behavior of silver nanomaterials in aquatic environments: An updated review. *Science of The Total Environment*, 167861 (2023). http://doi.org/10.1016/j.scitotenv.2023.167861
40. Estrada-Mendoza, T. A., Willett, D. & Chumanov, G. Light Absorption and Scattering by Silver/Silver Sulfide Hybrid Nanoparticles. *The Journal of Physical Chemistry C* 124, 27024–27031 (2020). http://doi.org/10.1021/acs.jpcc.0c08247

# Figures



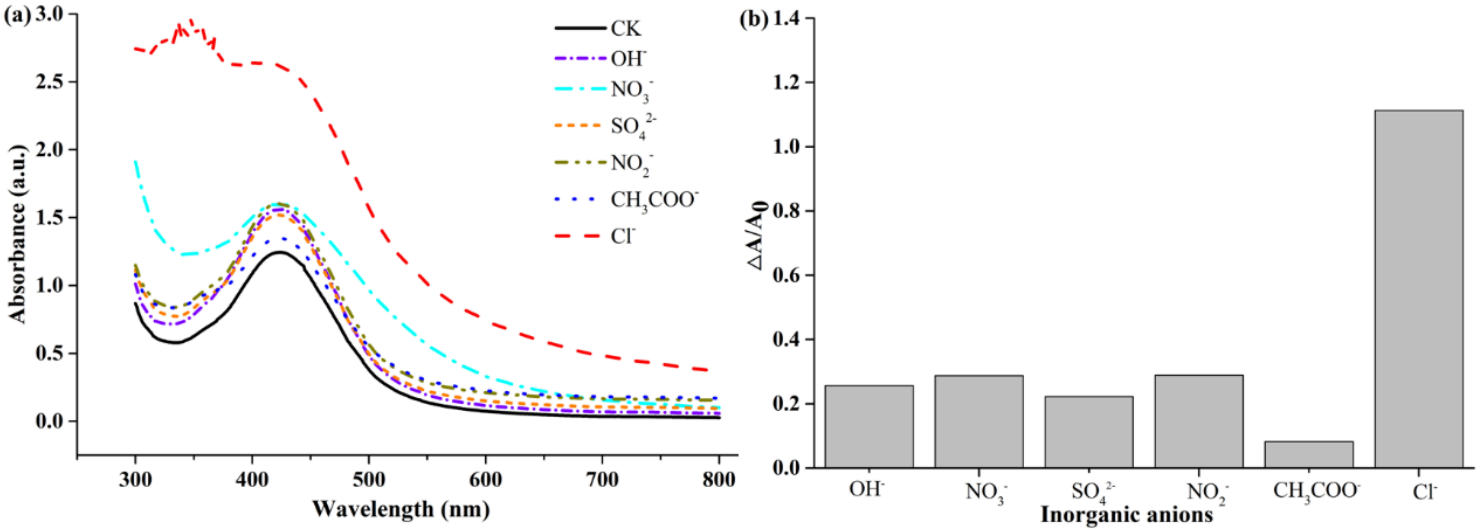

## Figure 1

Characterization of UV-vis spectra (a) and bacteriostatic properties (b) of AgNP.



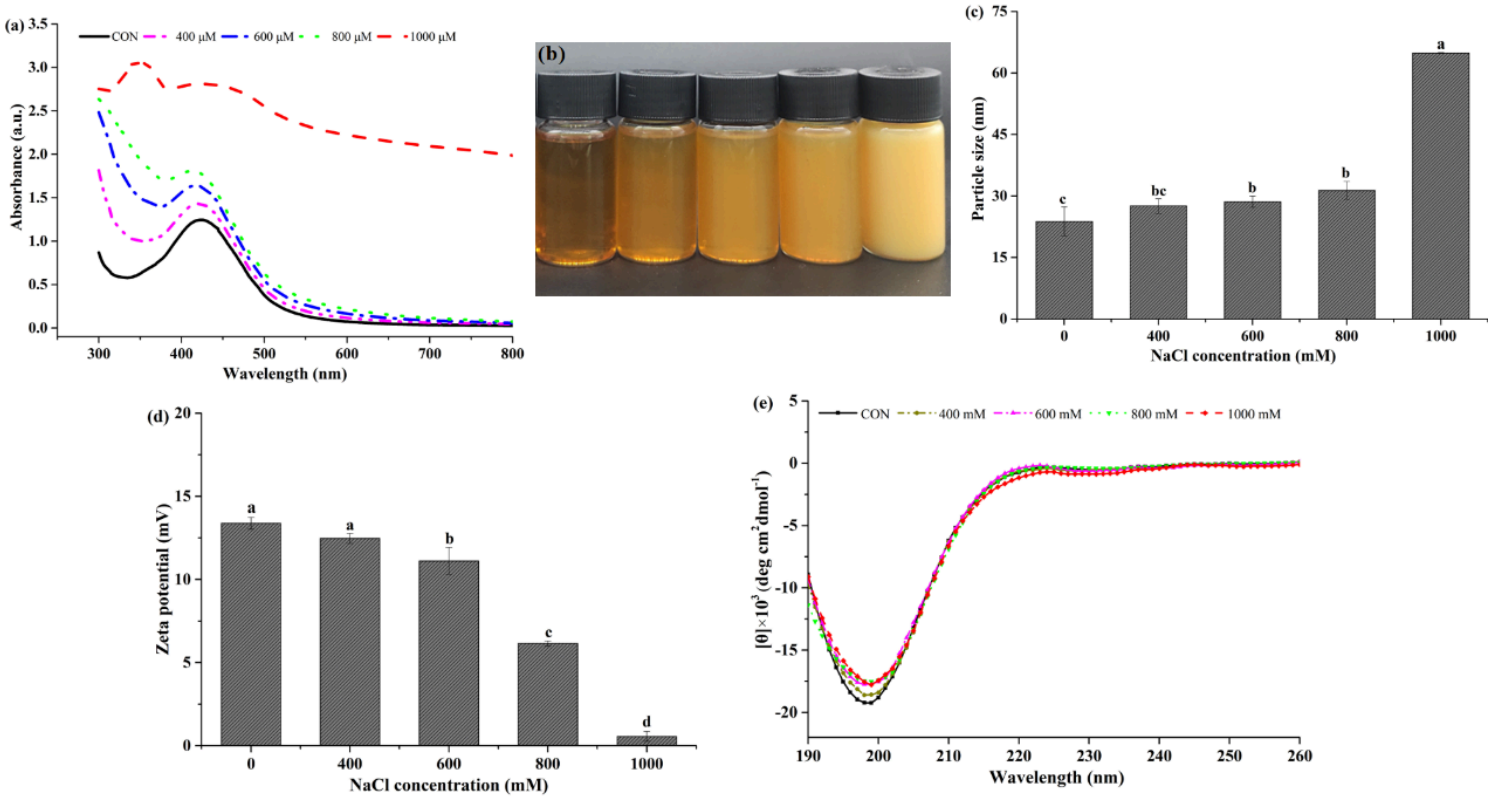

## Figure 2

Effect of AgNP on total colony count (a) TVB-N (b) and pH (c) of braised chicken meat during storage.




## Figure 3

Changes in UV-vis spectra (a) and selectivity (b) of AgNP after reaction with $Cl^-$ and other competing anions.




## Figure 4

Changes in UV-Vis spectra (a) color (b) particle size (c) zeta potential (d) and CD spectra (e) of AgNP reacted with different concentrations of NaCl.

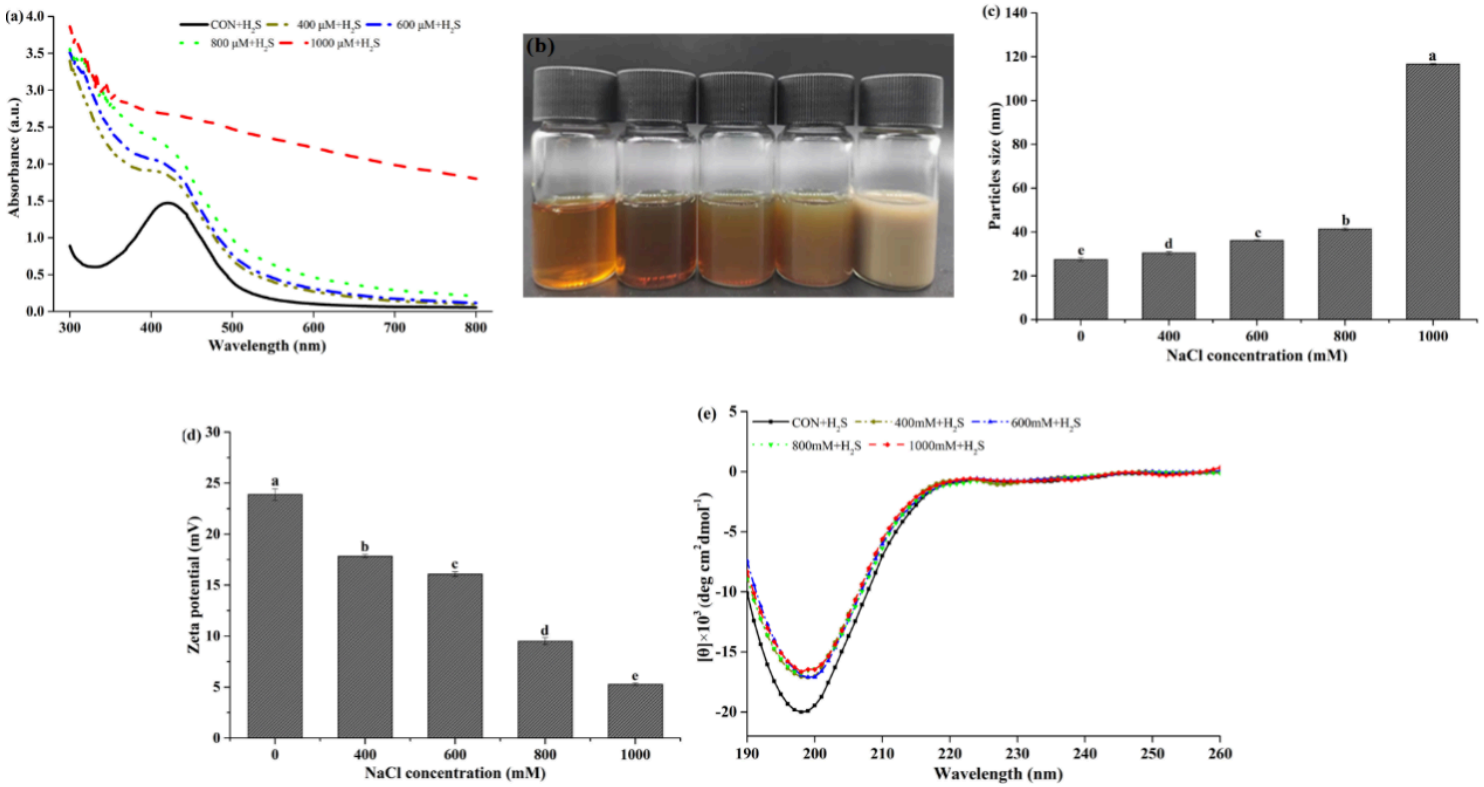



**Figure 5**

Changes in UV-Vis spectra (a) color (b) particle size (c) zeta potential (d) CD spectra (e) of AgNP reacted with different concentrations of NaCl and $H_2S$.

## Supplementary Files

This is a list of supplementary files associated with this preprint. Click to download.

- suppfigtable.docx
- Highlights.docx
- Graphicalabstract.docx